JOURNAL OF MATERIALS SCIENCE 29 (1994) 352–355

New evaluation technique of interfacial properties in GFRP

H. HAMADA, N. NISHIDA, Z. MAEKAWA
Faculty of Textile Science, Kyoto Institute of Technology, Matugasaki, Sakyo-ku, Kyoto 606, Japan

N. IKUTA
Osaka Municipal Technical Research Institute, Morinomiya, Jyoto-ku, Osaka 536, Japan

A new method was proposed to evaluate the mechanical properties at the interface between the fibres and the matrix in composites using an embedded single fibre coupon test. A mechanical parameter at the interface (called the interfacial transmissibility, κ) was derived from the fibre strength and the apparent stress of the fibre immediately before the first fracture of embedded fibre, σ_{fa}. This parameter indicated the degree of the mechanical transmission from the matrix to the fibre through the interface. This avoided some complicated problems such as the stress distribution along fibre fragments and the critical fragment state in a typical single-fibre test. This new method was tried to determine the κ-values for a fibre glass/epoxy resin with different amounts of a coupling agent at the interface. In order to measure the stress at the first fracture, the fracture process was monitored with a video camera during the single fibre test. The stress values at the first fracture for many coupons were analysed as a function of the three-parameter Weibull distribution. The resulting average stress and its coefficient of variation indicated that the reliability of the measurement for the stress at the first fracture was not less than that obtained by the usual single-fibre test. The change of interfacial transmissibility with amount of the coupling agent revealed the existence of an optimal interface.

1. Introduction

Embedded-single-filament coupon tests have been employed to evaluate interfacial shear strength [1–4]. In this technique a critical fibre length has to be measured [5]. When tensile strain is applied to the coupon, a number of fractures of embedded fibres occur. It is said that fibre is not cut in shorter when enough strain is applied. Then the fracture length is correlated to the critical fibre length.

However, this technique has some problems. In a previous article, the effects of pre-tension on the fracture state and fracture stress were discussed [6]. Here, pre-tension means that a load is subjected to a filament prior to embedding. The fracture begins at a lower stress since the pre-tension is higher. Therefore, it is difficult to judge the critical state. The other difficulty is that the calculation of interfacial shear strength is based on an assumption of a plastic model of interphase [7, 8]. In order to clarify whether the assumption is reasonable, the fracture process was observed during the tensile test. Finally, it was concluded that it was impossible to evaluate the interfacial shear strength from the critical fibre length, because the critical fibre length differed little with various surface treatments. Interfacial reinforcement by silane treatment affects the fracture process rather than the critical fibre length. It was necessary to propose a new analysis in the fracture process.

In this paper, the method of observing the fracture process is described in detail. The fibre-fracture process was analysed using a video-recording system and an image processor during the tensile test. Effects of the gauge length, tensile rate and fibre continuity on interfacial properties are discussed for this system. Finally, an Interfacial-Transmissibility parameter is proposed to describe the interfacial strength between the matrix resin and the fibre. This interfacial transmissibility is theoretically determined from the first fracture state. Furthermore, the silane treatment was examined to see how it affected the interfacial transmissibility.

2. Interfacial-transmissibility theory

Assume that the strain, ε_m, is applied to the matrix as shown in Fig. 1. If the fibre and matrix are completely bonded at the interface, the strain applied to the matrix is completely transmitted to the fibre. Then the strain of the fibre is equal to that of the matrix.

$$\varepsilon_f = \varepsilon_m$$

where ε_f is the strain of the fibre. The stress of the fibre is calculated from the stress of the matrix and the elastic moduli of the fibre and the matrix

$$\sigma_f = \sigma_m E_f/E_m \quad (1)$$

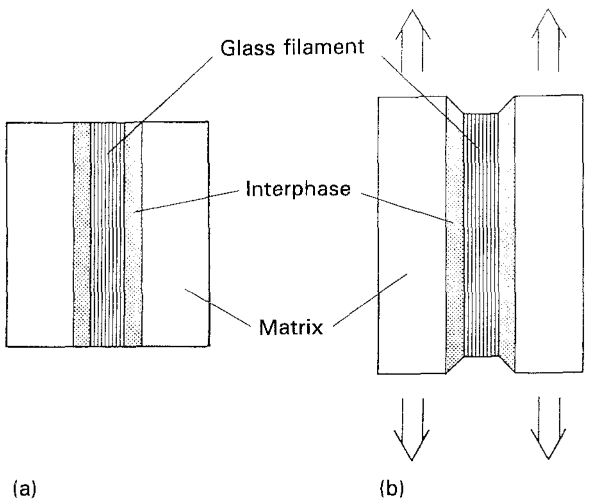

Figure 1 Schematic diagrams of an unloaded and a loaded specimen.

where σ_f is the stress of the fibre. If the interface cannot completely transmit strain

$$\varepsilon_f = 0$$

then,

$$\sigma_f = 0$$

Therefore, the ratio of ε_m and ε_f, κ, can be regarded as a coefficient of strain transmissibility at the interface.

$$\kappa = \varepsilon_f/\varepsilon_m \qquad (2)$$

So the bonding property of the interface can be evaluated with this equation by measuring the strains of the matrix and embedded fibre. However, it is difficult to measure the strain of an embedded fibre which is about 20 μm in diameter. The following equation can be obtained by the relation between stress, strain and elastic modulus.

$$\kappa = E_m\,\sigma_f/E_f\,\sigma_m \qquad (3)$$

where σ, ε and E are the stress, strain and elastic modulus, respectively. As this model is regarded as a unidirectional composite in which the fibre-volume fraction is nearly equal to 0, σ_m can be treated as follows

$$\sigma_m = \sigma_c \qquad (4)$$

where the suffix c denotes a composite. By substituting Equation 4 into Equation 3, κ is

$$\kappa = E_m\,\sigma_f/E_f\,\sigma_c \qquad (5)$$

The stress of the embedded fibre cannot be exactly measured. Therefore, the first fibre fracture was focused in the fracture process. The stress of the embedded fibre, σ_f, is equal to the fibre strength, s_f, at the first fibre fracture. In this experiment, a certain stress, T, was applied to the fibre during preparation of the specimen. Hence, the following equation can be obtained.

$$\sigma_f + T = s_f$$

$$\sigma_f = s_f - T \qquad (6)$$

By substituting Equation 6 into Equation 5, κ can be given as

$$\kappa = E_m\,(s_f - T)/E_f\,\sigma_c \qquad (7)$$

where terms excepted $s_f - T$ can be given as

$$\sigma_{fa} = \sigma_c\,E_f/E_m \qquad (8)$$

then if σ_{fa} is compared with σ_f in Equation 1, it is clear that σ_{fa} is the apparent stress of the fibre, on the assumption that the interface is completely bonded.

In this study, κ is named the interfacial transmissibility. It can be obtained by measuring the fibre strength and the coupon stress at the first fibre fracture.

3. Experimental procedure

3.1. Silane treatment

The glass fibre used in this study was an E-glass filament of 24 μm diameter. The filament was obtained from an E-glass yarn (2000 filaments/yarn) supplied by Nippon Glass Fibre. Prior to use, the yarn was heat cleaned at 600 °C for 2.5 h to remove binders and any other organic impurities. The silane coupling agent, γ-anilinopropyltrimethoxysilane (AnPS) was purchased from Shin-etsu Chemical Industry. The silane agent was used without further purification.

For silane treatment, a silane-coupling-agent solution was prepared by hydrolysing and dissolving an amount of AnPS in aqueous, 0.2 M acetic-acid solution. The silane concentration was changed from 0 to 2% to change the amount of silane on the glass surface. The E-glass yarn was immersed in the coupling-agent solution, and then cured at 90 °C for 20 min. The silane-treated filament was used to make specimens of the single-filament composites.

3.2. Preparation of specimens

The matrix material used in this study was a bisphenol-A-type epoxy resin (Epikote 828, Yuka-shell). The resin was mixed with 11 parts of a hardening

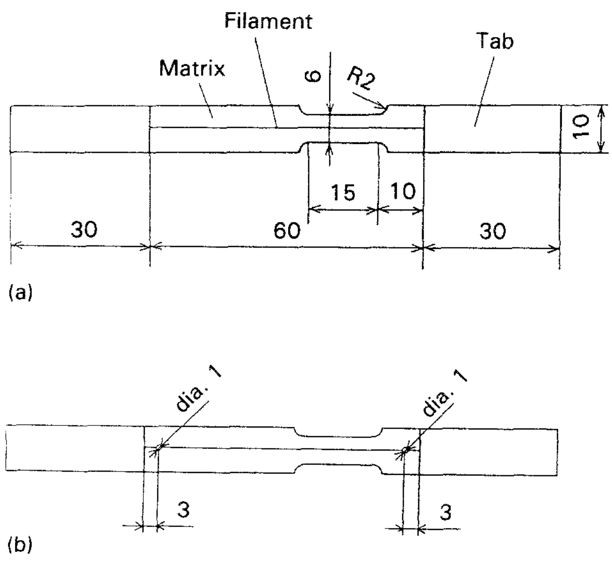

Figure 2 Dimensions of the specimens.

catalyst, triethylenetetoramine. The mixture was agitated thoroughly and then defoamed in a vacuum for approximately 10 min. This mixture was poured into a mould holding a glass filament with 10 gf in tension and subjected to curing at 50 °C for 80 min and post curing at 100 °C for 60 min. Fig. 2a shows the dimensions of the specimens. The dimension of the mould resulted in a specimen 1 mm thick, 6 mm wide, with a gauge length of 5, 15 and 25 mm.

In the embedded-single-filament coupon test, an ideal specimen has no embedded filament in the tab area. The embedded filament can have the applied load transmitted from the matrix through the interface. If the embedded filament exists in the tab area, the excessive stress may influence the fracture of the embedded filament. Fig. 2 shows two kinds of specimens; one is a specimen with no holes the other is a specimen with holes.

3.3. Measurement of the fracture process

The fracture points of the embedded filament were recorded with a video recorder during the tensile test. The view of the charge-coupled-device (CCD) camera was large enough to observe whole gauge area. The optical system was located across the specimen, as shown in Fig. 3. Fracture points along the fibre were detected by reflection of light from fracture cracks of the glass fibre. The fracture point can be determined at any time using an image processor (PIAS LA-500) combined with a computer (PC9801-VX, Nippon Electric Company).

Fig. 4a shows an example of the fracture state of a filament in a specimen; the light points are fibre fracture points, and the fibre had thirteen fracture points. Fig. 4b shows the brightness obtained by using an image processor along the fibre. The number of peaks was equal to the number of fracture points. The number of fracture points was continuously measured by the image processor until breakage of the specimen. The mean fragment length was evaluated from the number of fractures and the gauge length.

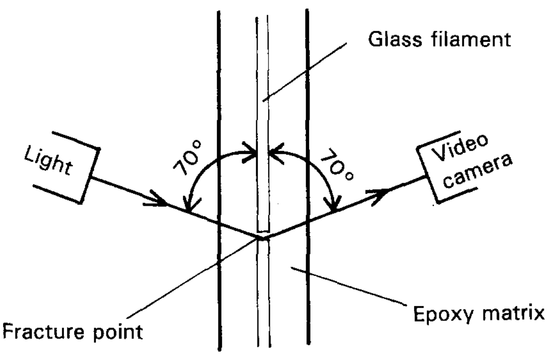

Figure 3 An optical system for detecting the fracture crack of a glass fibre.

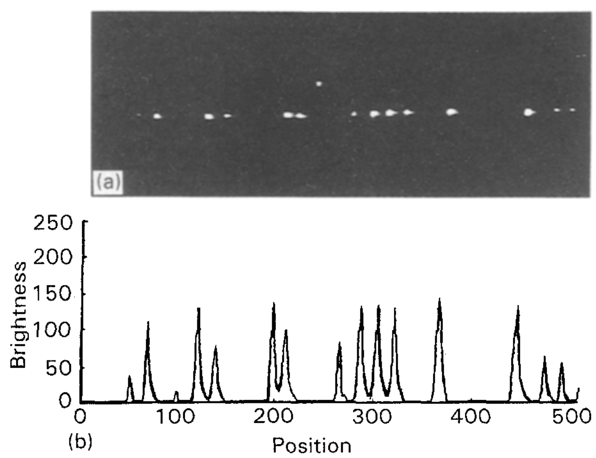

Figure 4 (a) Fracture state of a filament in a specimen, and (b) the brightness along the fibre.

4. Results and discussion

Fig. 5 shows the fracture process in each specimen as a plot of the mean fragment length against the stress of the specimen. The mean fragment length decreases with increasing stress. The fibre strength is generally given by a Weibull distribution. In the same manner, the distribution of the stress at the first fibre fracture was analysed. Fig. 6 shows the cumulative Weibull probabilities of σ_f and σ_{fa}. The value of κ was calculated from the mean value of σ_f and σ_{fa} as shown in Equation 7. The mean value was obtained by 50% of probability for Weibull distribution.

Table I shows the coupon stress at the first fibre fracture and the mean fragment length at the final

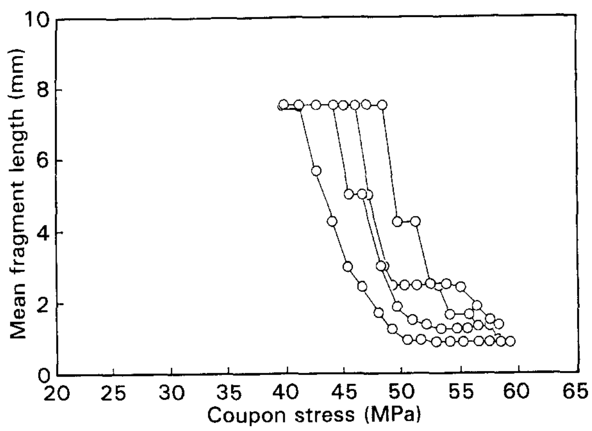

Figure 5 Changes of mean fragment length with coupon stress.

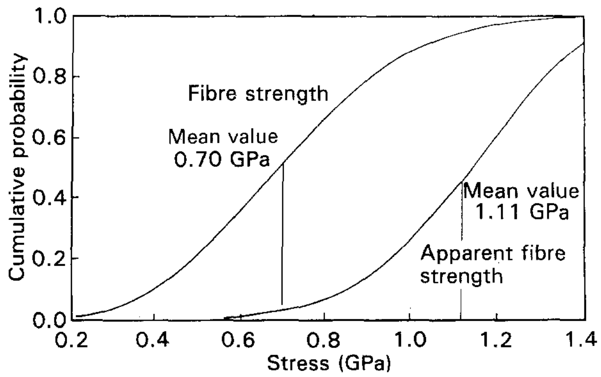

Figure 6 Cumulative probability curves of the fibre strength and the apparent fibre strength.

TABLE I Stress at the first fibre fracture, σ_{fp}; mean fragment length $\bar{l}$; and c.v. of both values at different gauge lengths

	Gauge length (mm)		
	5	15	25
σ_{fp} (MPa)	51.70	50.79	45.76
c.v. (σ_{fp})	0.224	0.107	0.222
$\bar{l}$ (mm)	3.10	5.94	13.24
c.v. ($\bar{l}$)	0.203	0.572	2.510

TABLE II Stress at the first fibre fracture, σ_{fp}; mean fragment length $\bar{l}$; and c.v. of both values at different crosshead speeds

	Crosshead speed (mm min^{-1})		
	0.6	1.0	3.0
σ_{fp} (MPa)	46.50	50.79	46.99
c.v. (σ_{fp})	0.108	0.107	0.172
$\bar{l}$ (mm)	4.92	5.94	4.47
c.v. ($\bar{l}$)	0.497	0.572	0.477

TABLE III Stress at the first fibre fracture, σ_{fp}; mean fragment length $\bar{l}$; and c.v. of both values in the cases of specimens with no hole and with holes

	No hole	Hole
σ_{fp} (MPa)	45.90	44.23
c.v. (σ_{fp})	0.060	0.067
$\bar{l}$ (mm)	2.35	1.847
c.v. ($\bar{l}$)	0.660	0.379

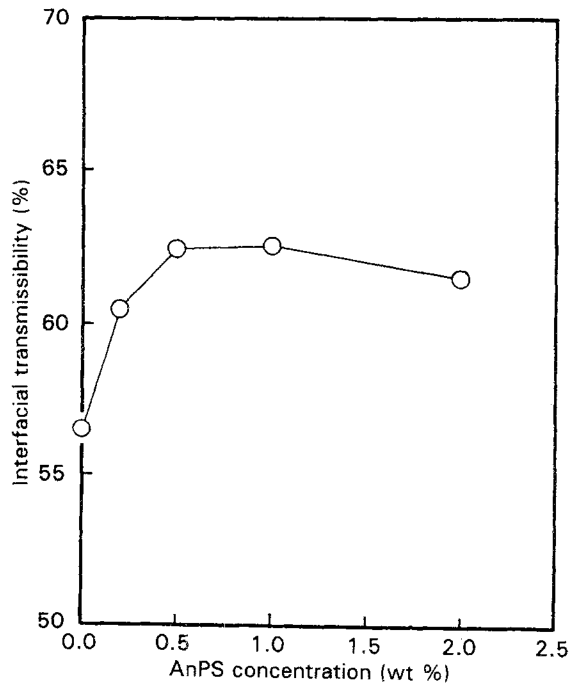

Figure 7 Change of interfacial transmissibility with AnPS concentration.

state, which was immediately before the breakage of the specimen for gauge lengths of 5, 15, and 25 mm. The coefficient of variation (c.v.) of both values are also listed in Table I. The mean fragment length varied greatly compared with the stress at the first fibre fracture.

Table II shows another result for crosshead speeds of 0.6, 1, and 3 mm min^{-1}. In this result, the test speed had little influence on the mean fragment length and the coupon stress at the first fibre fracture.

Table III shows the effect of the hole. In this result, the existence of the hole had little influence on the mean fragment length and the coupon stress at the first fibre fracture. The mean fragment length varied greatly compared with the stress at the first fibre fracture by test conditions.

Fig. 7 shows the interfacial transmissibility calculated from the values of σ_{fa} and σ_f as a function of silane concentration in the treatment. In this examination, a gauge length of 15 mm and a crosshead speed of 1 mm were employed as test conditions. These conditions had the minimum c.v. value, as seen in Table I and II. The interfacial transmissibility gave maximum values around 0.5 w/w% for the AnPS solution. This result means that the silane concentration should be optimized to get the best interfacial strength. The reason for the optimum concentration and the relation between the chemical bonding structure at the interface and the interfacial transmissibility will be discussed in a future paper.

5. Conclusion

An embedded-single-filament coupon test was carried out. Interfacial transmissibility was proposed as a parameter of interfacial strength by the first fracture stress. As a result, the c.v. of the first fracture stress had a small value and was little influenced by the test conditions. It was suggested that the evaluation by the first fracture stress was a valid way of evaluating the interfacial strength.

References

1. A. KELLY and W. R. TYSON, *J. Mech. Phys. Solid* **13** (1965) 329.
2. V. RAO and L. T. DRZAL, *Polym. Compos.*, **12** (1991) 1.
3. N. IKUTA, Z. MAEKAWA, H. HAMADA, S. YOSHIOKA, and T. HIRASIMA, "Interface in polymer, ceramic, and metal matrix composites", edited by H. Ishida, (Elsevier, New York, 1988) p. 611.
4. N. IKUTA, H. HAMADA, Z. MAEKAWA, S. YOSHIOKA, and T. HIRASHIMA, Japan–US Conference on composite materials, Washington DC, June 27–29 (Technomic, Pennsylvania, 1988) p. 222.
5. L. T. DRZAL, M. J. RICH, and P. F. LLOYD, *J. Adhesion*, **16** (1982) 1.
6. N. IKUTA, Z. MAEKAWA, H. HAMADA, H. ICHIHASHI, and E. NISHIO, *J. Mater. Sci.* **26** (1991) 4663.
7. A. KELLY and G. J. DAVIES, *Metallurgical Rev.* **10** (37) (1965) 1.
8. L. T. DRZAL, NASA Conference Publication No. NASA-CP-2334, (1984) p. 227.

Received 8 May 1992
and accepted 3 February 1993